Starting Characteristic Analysis of LSPM for Pumping System Considering Demagnetization

Subrato Saha, Yun-Hyun Cho

Abstract—This paper presents the design process of a high performance 3-phase 3.7 kW 2-pole line start permanent magnet synchronous motor for pumping system. A method was proposed to study the starting torque characteristics considering line start with high inertia load. A d-q model including cage was built to study the synchronization capability. Time-stepping finite element method analysis was utilized to accurately predict the dynamic and transient performance, efficiency, starting current, speed curve and etc. Considering the load torque of pumps during starting stage, the rotor bar was designed with minimum demagnetization of permanent magnet caused by huge starting current.

Keywords—LSPM, starting analysis, demagnetization, FEA, pumping system.

I. INTRODUCTION

RECENTLY due to the demand of energy saving purpose, replacement of the line-operated induction motor (IM) by line start permanent magnet synchronous motor (LSPM) is of concern in both academy and industry. LSPM has a higher efficiency than (IM) and an advantage in constant speed operation regardless of the effect of load variation, presenting an interesting alternative for IMs in pumping systems. It has permanent magnets (PMs) buried bellow the squirrel cage in rotor, thus operates in steady state as conventional interior permanent magnet synchronous motor (PMSM) [8]; the squirrel cage is used for line starting on a conventional AC power source and damping of dynamic oscillations at fast load changes. Thus it combines the advantages of induction motor (robust construction and line-starting capability) and PMSM (high efficiency, power factor and torque density). So, characteristics of LSPM have very complex characteristics until the synchronization and if the design is not suitable, the LSPM cannot be synchronized [1]-[2].

The breaking torques (due to permanent magnets and flux barriers) in the asynchronous operation region, which mainly depends on the placement and dimensions and the value of energy product of PMs and the value of energy product of PMs, has principle effect on the synchronization capability [9], [10]. The design of high performance motor should make compromise between an adequate staring characteristic in the asynchronous operating region and power rating and efficiency in the motor's synchronous operating region [3]. In

SubratoSaha is with the Dong-A University, Busan, 604-714, South Korea. He is now with the Department of Electrical Engineering (e-mail: shuvo4279@gmail.com).

Yun Hyun Cho is Honorable Professor with the Electrical Engineering Department, Dong-A University, Busan, 604-714 South Korea (Phone: +82-10-3285-7742, fax: +82-51-200-7743, e-mail: yhcho@dau.ac.kr).

this paper the pumping system was analyzed first to obtain load torque characteristic of motor. A 3-Phase 3.7KW 2-Pole LSPM was designed based on induction motor for the same pump set, with PM inserted under rotor bar and stack length reduced by 10%. In order to control cost, the thickness of PM was 2 mm, and it is easy to demagnetize during starting. In order to reduce the risk of PM demagnetization, the rotor bar was redesigned to reduce starting current, while matching pump requirement. A d-q model including cage was built to study the synchronization capability, and time stepping finite element method (FEM) was used to analyze the performance of starting and synchronous operation.
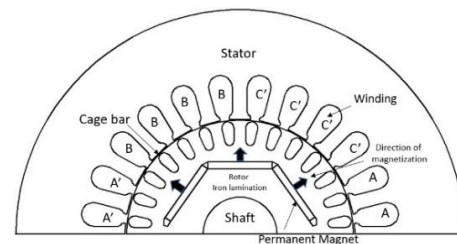

Fig. 1 Configuration of a three phase 2 pole LSPM

TABLE I
DESIGN SPECIFICATION OF LSPM

Symbol	Item	Value
-	Phase	3
-	Pole Number	2
T_r	Rated Torque [Nm]	9.8
n_r	Rated Speed [rpm]	3600
f	Frequency [Hz]	60
D_{so}	Stator Outer Diameter [mm]	159
D_{si}	Stator Inner Diameter [mm]	89
L_m	Lamination [mm]	90
D_{ro}	Rotor Outer Diameter [mm]	87.8
D_{ri}	Rotor Inner Diameter [mm]	25.4
R_b	Rotor bar number	28
R_m	Rotor bar material	Al
PM	Material of magnets	Nd-Fe-b
-	Stack Length [mm]	90
-	Br at 100°C [T]	1.21
-	Hc at 100°C [KA/m]	7.35
-	Thickness [mm]	3
V	Voltage[v]	380
-	Connection	Y
P	Rated power[w]	3700
-	Core material	S23

World Academy of Science, Engineering and Technology
International Journal of Mechanical and Mechatronics Engineering
Vol:9, No:7, 2015

II. CHARACTERISTICS OF PUMPING SYSTEM

A pump converts mechanical energy into pressurized fluid motion to move liquids through a piping network. Impeller rotating adds energy to fluid that enters the center or eye of the rotating impeller. The fluid is then acted upon by centrifugal force of the impellor, or tip speed force. These forces result in an increase in the pressure and velocity of the fluid. Fig. 2 depicts a typical pumping system head curve, or system curve. The three components of total system head are static head, design working head, and friction head. Static head is the vertical difference between the system's point of entry and its highest point of discharge. Design working head is that head that must be available at a specified location to satisfy design requirements. Friction head is the head required by the system to overcome the resistance to flow in pipes, valves, fittings and mechanical equipment. Pump manufacturers provide pump head-capacity that predict pump performance, often shown as a single-line curve depicting one impeller diameter or as multiple curves for the performance of several impeller diameters in one casting. A pump operates over a range of pressure or head and flows for a given speed and impeller diameter.

A system curve can be developed and overlaid on the pump curve. The system curve represents how the piping network responds to varying flow and pressure. The intersection of the pump head-capacity curve and the system curve represents the operating point of the pump for a specific piping system. This condition represents the point at which pump head matches the system head as defined by the system piping configuration. The mechanic output power of a pump is given by

$$P(W) = H(m) \times Q(kg/s) \times 9.81(m/s^2) \times \frac{1}{\eta} \quad (1)$$

where H is head and Q is flow rate.

Head varies as the square of the rotating speed, and flow (capacity) varies with rotating speed N (i.e., the peripheral velocity of the impeller). Thus, the brake power varies as the cube of the rotating speed
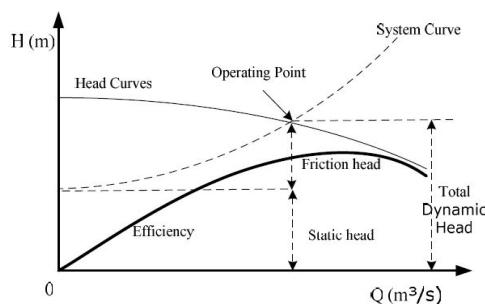

Fig. 2 System curve and pump curve

The load torque is proportional to square of the rotating speed, means that, the load torque is relative small at starting, which is quite different with traction applications which needs rated torque at low speed.

III. BASIC THEORY FOR STARTING ANALYSIS

A. Analysis of Starting

The equation for stator voltage is given as [4]

$$V \sin\delta = p\lambda_d - \lambda_q\omega_r + R_s i_d ,$$
$$V \cos\delta = p\lambda_q + \lambda_d\omega_r + R_s i_q \quad (2)$$

Here R_s is the phase resistance of stator winding, $p = \frac{d}{dt}$.

Voltage equation of rotor can be written as

$$0 = p\lambda_{2d} + R_d i_{2d} ,$$
$$0 = p\lambda_{2q} + R_d i_{2q} , \quad (3)$$

The permanent magnet may be modeled by a rotor coil with dc excitation current, I_{fm} such that

$$I_{fm} = \frac{E_0}{X_{md}} \quad (4)$$

The flux linkage equations can be written as

$$\lambda_d = L_d i_d + L_{md} i_{2d} + L_{md} I_{fm}$$
$$\lambda_q = L_q i_q + L_{md} i_{2q}$$
$$\lambda_{2d} = L_{2d} i_{2d} + L_{md} i_d + L_{md} I_{fm}$$
$$\lambda_{2q} = L_{2q} i_{2q} + L_{mq} I_q \quad (5)$$

where d, q axis inductances can be related to stator and rotor leakage inductances as

$$L_d = L_{md} + L_1 \quad L_q = L_{md} + L_1$$
$$L_{2d} = L_{md} + L_2 \quad L_{2q} = L_{mq} + L_2 \quad (6)$$

Here L_1 and L_2 are the leakage inductance of stator and rotor.

$$V_d = (R_s + pL_d)i_d - \omega_r L_q i_q + pL_{md}i_{2d} - \omega_r L_{mq}i_{2q} + pL_{mq}i_{fm}$$
$$V_q = \omega_r L_d i_d + (R_s + pL_q)i_q + \omega_r L_{mq}i_{2q} + pL_{mq}i_{2q} + \omega_r L_{mq}i_{2q}$$
$$0 = pL_{md}i_d + (R_d + pL_{2d}) + pL_{md}i_{fm}$$
$$0 = pL_{mq}i_q + (R_q + pL_{2q})i_{2q} \quad (7)$$

The instantaneous rotor acceleration is given as

$$\frac{d\omega_r}{dt} = \frac{P}{2J}(T_e - T_L) \quad (8)$$

where P is the number of poles is rotor angular speed, J is the number of rotor inertia, T_L is the load torque and T_e is the electromagnetic torque. The total electromagnetic torque developed at sub-synchronous speed is composed of two components namely, the cage torque due to the rotor squirrel cage winding and the magnet break torque due to the permanent magnet excitation. The rotor cage torque is given as:

World Academy of Science, Engineering and Technology
International Journal of Mechanical and Mechatronics Engineering
Vol:9, No:7, 2015

$$T_c = \frac{P}{2}\frac{m}{\omega_s}\left\{\begin{array}{l}\left(X_{2d}-X_{2q}\right)I_{2d}I_{2q}+X_{md}I_dI_{2q}\\ -X_{mq}I_qI_{2d}+E_0VI_{2q}\end{array}\right\} \qquad (9)$$

The braking torque due to permanent magnet is given by

$$T_m = \frac{P}{2}\frac{m}{\omega_s}\left\{X_{md}I_{fm}I_{md}+\left(X_d-X_q\right)I_{md}I_{mq}\right\} \qquad (10)$$

Total electromagnetic torque T_e is given as

$$T_e = \frac{P}{2}\frac{m}{\omega_s}\left\{\begin{array}{l}\left(X_d-X_q\right)I_dI_q+X_{md}I_{2d}I_q\\ -X_{mq}I_{2q}I_q+E_0I_q\end{array}\right\} \qquad (11)$$

During asynchronous operation, the magnet torque has a pulsating component with frequency $s.f_s$, where s is the slip between the stator rotating field and rotor movement, and the torque curves according to speed are plotted in Fig. 3. The dot curve is the torque that would be obtained without the magnet braking torque and the solid curve is the net average torque. The braking torque is due to the generating action of the magnets, which give rise to a component of stator current that produce resistive losses in the stator circuit resistance [2]. During steady state, the torque is given in terms of currents by

$$T_{syn} = \frac{P}{2}\frac{m}{\omega}\left[E_0I_q+I_dI_q\left(X_d-X_q\right)\right] \qquad (12)$$

In terms of voltage, if δ is the angle between the EMF and the terminal voltage, neglecting resistance,

$$T_{sys} = \frac{P}{2}\frac{m}{\omega}\left\{\frac{E_0V_{ph1}}{X_d}\sin\delta+\frac{V_{ph1}^2}{2}\left(\frac{1}{X_q}-\frac{1}{X_d}\right)\sin 2\delta\right\} \qquad (13)$$
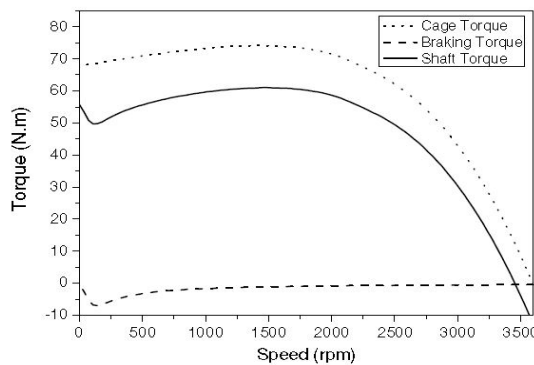
$$= T_1\sin\delta+T_2\sin 2\delta$$


Fig. 3 Starting Torque for LSPM

IV. STARTING PERFORMANCE

The starting performance of original model was studied with the aid of computed transient torque/speed and related trajectories. At no load state, the motor could synchronize to a steady speed of 3600rpm within 2S as given in Fig. 4. While under a load of 9.8N.m and inertia of 6 times of rotor, it takes about 1.6S for motor to reach steady speed. With a larger

inertia, the instantaneous speed/torque trajectory has a series of slow pole-slips in Fig. 5 (b) as almost elliptical cycles. It could be concluded that the original model has a relative high starting performance, but following the demagnetization problem of PM during starting caused by large starting current.
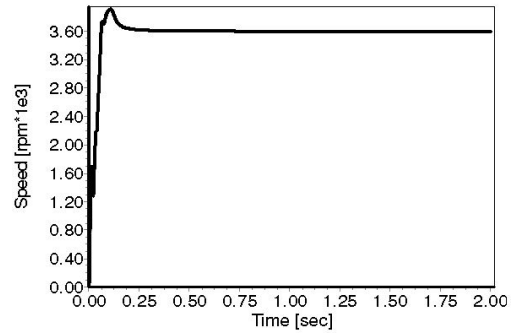
(a)
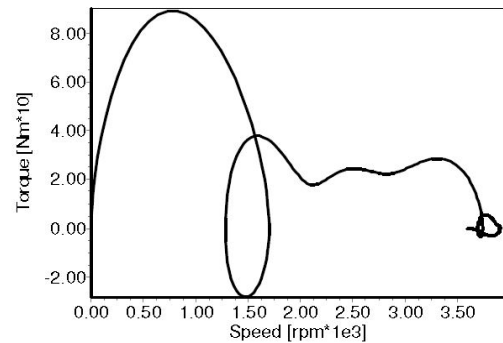
(b)

Fig. 4 3.7kW LSPM starting analysis, TL=0, J=1 p.u., (a) speed curve, (b) speed/torque trajectory

V. PERFORMANCE INVESTIGATION BY FEM

A. Analysis of Original Model

The original design derived from a standard 3.7kW IM was simulated by two-dimensional transient magnetic analysis using commercial software package Maxwell. Motor was fed with a 3-phase power source 380V, 60 Hz and started with full load 9.8N.m. The simulation model is given in Fig. 6, with rotor bar shape same as IM and three magnets inserted under rotor bar. The starting currents, torque curve and speed curve are illustrated in Fig. 7. Starting current reaches as high as 80A as shown in Fig. 7 (a), which causes demagnetization of PM. The permeance coefficient and flux density distribution of PM during starting was plotted in Fig. 8. The flux generated by the rotating magnetic field from armature opposes the flux of middle and left PM, the amount of armature flux caused by starting current surpassed PM flux by a large degree, would then causes irreversible demagnetization [5]. The demanded torque from pump is relatively lower during starting than synchronous speed. In order to reduce the starting current, the rotor bar size was reduced by 40% in the second prototype as shown in Fig. 9. The PM shape and flux barrier was also

World Academy of Science, Engineering and Technology
International Journal of Mechanical and Mechatronics Engineering
Vol:9, No:7, 2015

redesigned for cost reduction purpose [6]. The starting currents, torque curve and speed curve are illustrated in Fig. 10. The peak current decreased to 51A comparing with original model.
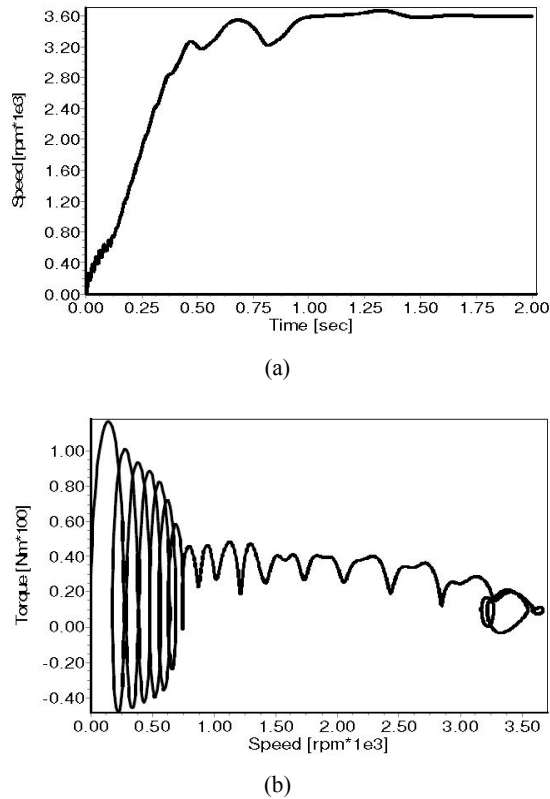

(a)

(b)

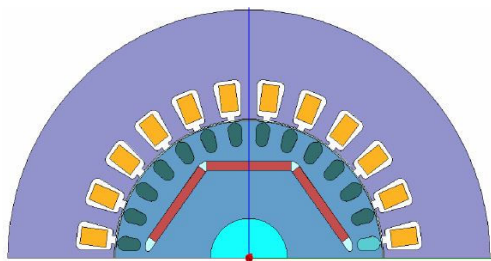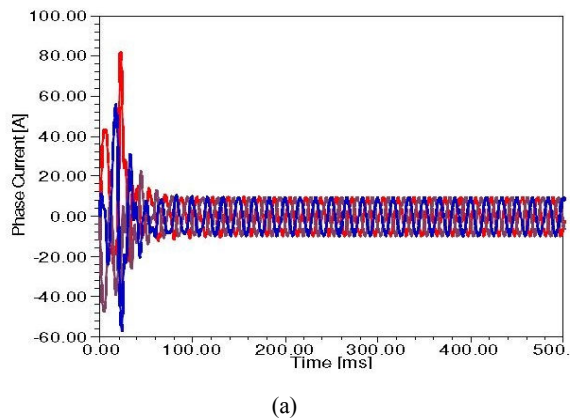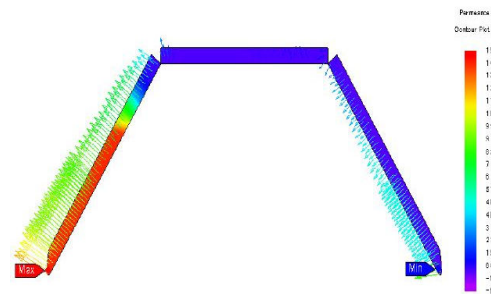Fig. 5 3.7kW LSPM starting analysis, TL=9.8N.m, J=6 p.u.,(a) speed curve, (b) speed/torque trajectory

Fig. 6 Original model simulation

(a)

(b)

(c)
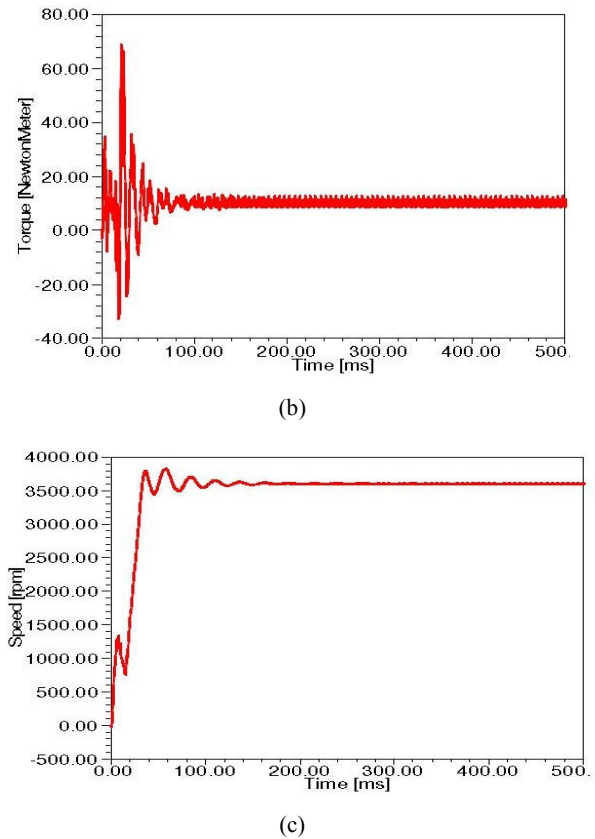
Fig. 7 Original model simulation (a) phase current (b) Torque (c) speed

Fig. 8 Permeance coefficient and flux density distribution
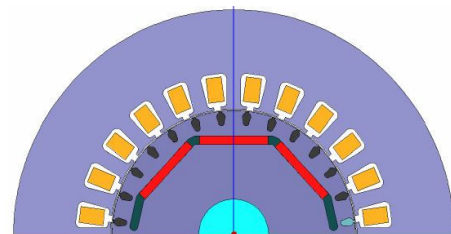
Fig. 9 Modified model simulation

World Academy of Science, Engineering and Technology
International Journal of Mechanical and Mechatronics Engineering
Vol:9, No:7, 2015
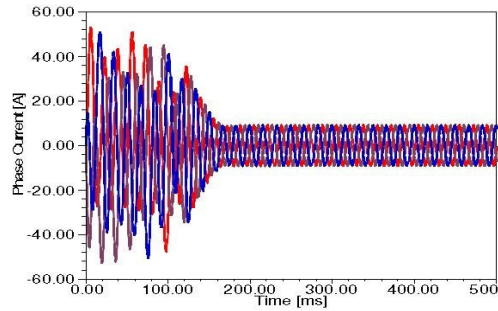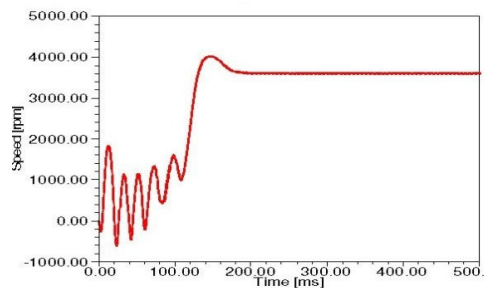
(a)
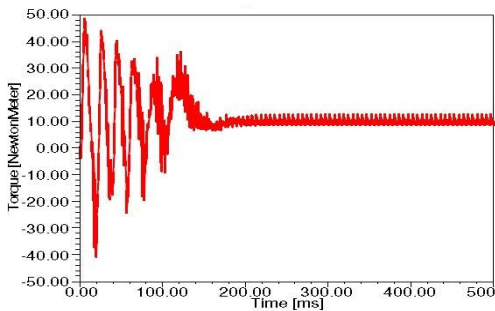
(b)

(c)

Fig. 10 Simulation results of modified model (a) Phase currents (b) Torque (c) Speed

VI. EXPERIMENT VALIDATION

Experiment was set up to test the prototype motors using dynamo test bed as shown in Fig. 11. Photo of two rotors from original model and modified model are given in Fig. 12. The performance curves according to different load torque at rated speed 3600rpm were summarized in Figs. 13 (a) and (b) [7]. The efficiency at rated torque 9.8 N.m is about 90%, which is about 2% higher than corresponding standard high efficiency induction motor. The designed motors also exhibit high efficiency with a large range of load. Prototype motors were assembled with pump to test the starting performance as shown in Fig. 14. The starting currents are illustrated in Fig. 15. The peak value of starting current during pump test was 87.5A and 27.5A for original model and modified model, respectively. The simulation result of modified model is 52A, 13.5A higher than experiment results. The simulation result of original model is 80A, 7.5A lower than simulation result. The difference was due to fact that initial position of rotor has a large influence on starting current.
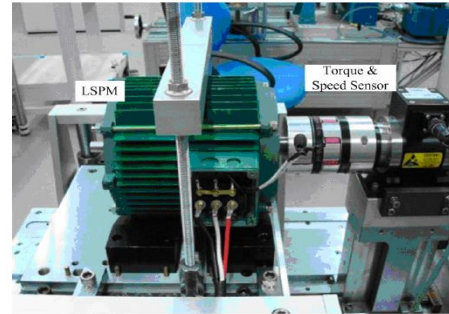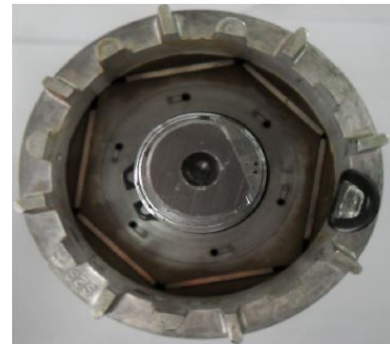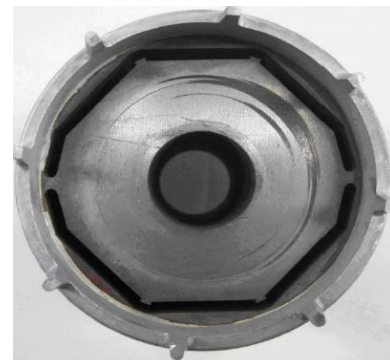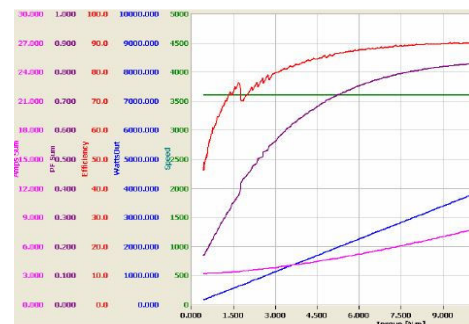
Fig. 11 Dynamo setup

(a)

(b)

Fig. 12 Rotor Prototype (a) original model (b) modified model

(a)

World Academy of Science, Engineering and Technology
International Journal of Mechanical and Mechatronics Engineering
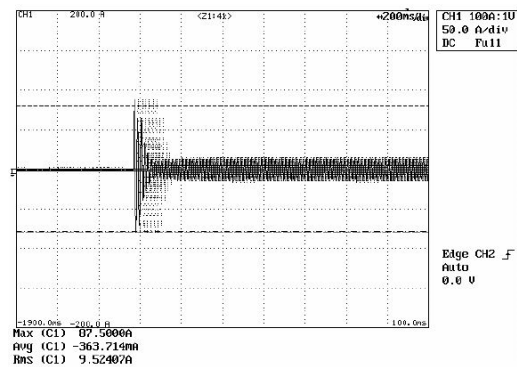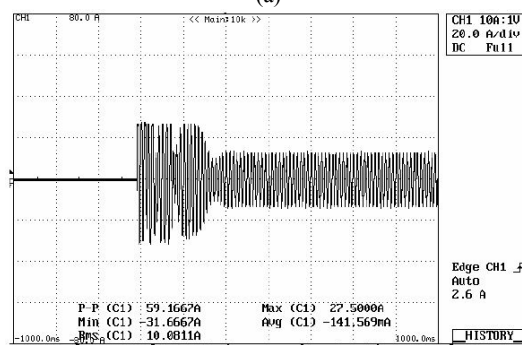Vol:9, No:7, 2015
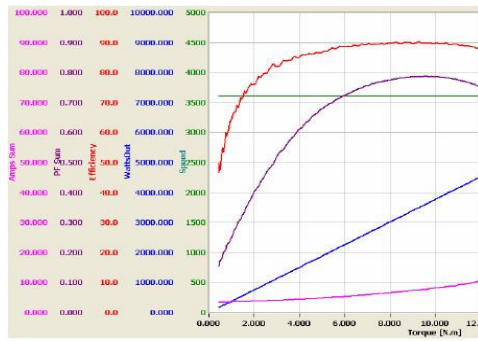
(b)

Fig. 13 Performance curves at rated speed (a) original model (b) modified model

Fig. 14 Experimental setup for pump test

(a)

(b)

Fig. 15 Starting current during pump test (a) original model (b) modified model

VII. CONCLUSION

This paper describes the developing process of a 3-Phase3.7kW 2-Pole LSPM for pumping system. Two dimensional transient finite element analysis was utilized for accurate calculation of efficiency, starting current speed curve and etc. Pumping system was analyzed first to obtain load torque characteristic of driving motor. In order to reduce the risk of PM demagnetization, the rotor bar was redesigned to reduce starting current, while matching pump requirement. A d-q model including cage was built to study the synchronization capability, and time-stepping FEM was used to analyze the performance of starting and synchronous operation. Dynamo test and pump test were carried out to measure the synchronous operation performance and starting performance. Experimental results and FEM result are matched, which verifies the validity of this analysis. The experimental results obtained from the prototype demonstrate satisfactory agreement with the estimated by FEA approaches, and underpin the findings of the study and optimum design for the rotor are satisfied with the required motor specification.

REFERENCES

[1] M.A Rahman and T.M. Osheiba, "Performance of a large line start permanent magnet synchronous motor", IEEE Trans. Energy Conversion, vol. 5, pp.211-217, Mar.1990.
[2] T.J.E. Miller, "Synchronization of line-start permanent magnet AC motor", IEEE Trans. Industry Application, vol.PAS-103, Juillet 1984, pp 1822-1828.
[3] Li Gies, GuoZhongbao, Wang Chunyuan, Giu Hong, GuoDaling, "High Starting Torque and High Efficiency REPM Synchronous Motor", Proceeding of the Seventh International Workshop on Rare Earth-Cobalt Permanent Magnets and Their Applications, Beijing, China, Sept. 1983, Chana Academic Publishers, pp.13-20.
[4] A. Takahashi, S. Kikuchi, K. Miyata, S. Wakui, H. Mikami, and A. Binder, "Transient-torque analysis for line-starting permanent-magnet synchronous motors", Proceeding of the 2008 International Conferences on Electrical Machines, Beijing, China, Sept. 1983, Chana Academic Publishers, pp.13-20.
[5] G.H. Kang, J. Hur, H. Nam, J.P. Hong and G.T. Kim "Analysis of irreversible magnet demagnetization in line-start motors based on the finite-element method", IEEE Trans. On Magn., vol.39, no.3, pp.1488~1491, May, 2003.
[6] W.H Kim, K.C Kim "A study on the optimal rotor design of LSPM considering the starting torque and efficiency", IEEE Trans. on magn., Vol.45,No.3, March 2009
[7] Tingting Ding , Takorabet N.,Sargos F-M, Xiuhe Wang, " Design and Analysis of different line start PM synchronous motor for oil-pump applications", IEEE Trans. on magn.,Vol.45, No.3, March 2009
[8] T. J. E. Miller, "Synchronization of line-start permanent magnet AC motors," IEEE Trans. Power App. Syst., vol. PAS-103, no. 7, pp. 1822–1828, Jul 1984.
[9] J. Soulard and H. P. Nee, "Study of the synchronization of line-start permanent magnet synchronous motors," in Proc. IEEE Ind. Applicat. Soc. Annu. Meeting, Roma, Italy, 2000, pp. 424–431.

[10] V. B. Honsinger, "Permanent magnet machines: Asynchronous operation," IEEE Trans. Power App. Syst., vol. PAS-99, no. 7, pp. 1503–1509, Jul. 1980.